

Gold(I)-induced chelate ring-opening of palladium(II) and platinum(II) triphos complexes

Paloma Sevillano,^a Abraha Habtemariam,^b Simon Parsons,^b Alfonso Castiñeiras,^a M. Esther García^{*a} and Peter J. Sadler^{*b}

^a Department of Inorganic Chemistry, University of Santiago de Compostela, E-15706 Santiago de Compostela, Spain

^b Department of Chemistry, University of Edinburgh, King's Buildings, West Mains Road, Edinburgh, UK EH9 3JJ. E-mail: P.J.Sadler@ed.ac.uk

Received 11th May 1999, Accepted 23rd June 1999

The complexes [M(triphos)Cl]Cl [triphos = PhP(CH₂CH₂PPh₂)₂; M = Pd (**1**), M = Pt (**2**)] undergo ring-opening reactions with Au(I) to give [MAu(triphos)Cl₃] [M = Pd (**3**), M = Pt (**4**)]. In these mixed metal complexes, triphos acts as a bidentate ligand for M and the third phosphorus atom is coordinated to Au(I) with a linear geometry. Complexes **1–4** were characterised by microanalysis, FAB mass spectrometry, IR, NMR (³¹P and ¹⁹⁵Pt) spectroscopies and conductivity measurements. Complexes **2–4** were also characterised by X-ray crystallography. [Pt(triphos)Cl]Cl, **2**, is monoclinic, space group *P2₁/n*, with square-planar geometry. The Pt–P_{central} bond distance (2.207 Å) is shorter than the other two Pt–P distances (2.312 and 2.315 Å). [PdAu(triphos)Cl₃], **3**, is also monoclinic (space group *P2₁/n*), with square-planar Pd(II) and linear Au(I) (P–Au–Cl 177.73°), and has a similar structure to complex **4**, [PtAu(triphos)Cl₃] (monoclinic, space group *I2/a*). The thiolate S of the tripeptide glutathione (GSH) and *N*-acetyl-L-cysteine binds to [Pt(triphos)]²⁺ giving adducts with high aqueous solubility. In the presence of Au(I), 5'-GMP displaced glutathione from [Pt(triphos)(GS)]⁺ to form two adducts. Both GSH and *N*-acetyl-L-cysteine readily extracted Au(I) from complex **4**, [PtAu(triphos)Cl₃], to give complex **2**, [Pt(triphos)Cl]Cl, and the Au(I) thiolate. Since chloride and thiolates would be strong competitors to DNA binding, proteins could be possible target sites for these complexes.

Introduction

A large number of polydentate phosphine complexes of transition metals have been synthesised and characterised which have potential applications in homogeneous catalysis and medicine.^{1–4} Chelating phosphine ligands are also useful for stabilising metal–metal bonds^{5,6,7} and can result in unusual coordination numbers and geometries.⁸ Chelation often prevents phosphine dissociation, in contrast to the behaviour of analogous complexes of monophosphine ligands.⁹

The interactions of bis(phosphino)complexes of platinum(II) with nucleic acid components,^{10,11} as well as analogous nucleobase complexes of Pt(II) and Pt(IV) amines have been studied.^{12,13} It has been shown that Pt(II) aminophosphine complexes can bind to the DNA bases guanine and thymine *via* ring-opening reactions and are cytotoxic to cancer cells.^{14,15} 1,2-Diphenylphosphinoethane (dppe) complexes of gold(I) exhibit anticancer activity against a range of tumours, while the triethylphosphine Au(I) complex auranofin is used as an antiarthritic drug.² The combination of square-planar Pt(II) and linear Au(I) centres in a single complex, as investigated in the present work, may therefore give rise to interesting biological activity.

In our previous work on triphos complexes (triphos = bis[2-(diphenylphosphino)ethyl]phenylphosphine), we have shown that chelate ring-opening of [Pd(triphos)Br]Br can be induced by oxidizing agents giving the square-planar Pd(II) complex [Pd(Ph₂P(O)CH₂CH₂P(Ph)CH₂CH₂PPh₂)₂][PdBr₄], or the unusual square-pyramidal five-coordinate Pd(II) complex, [Pd(Ph₂P(O)CH₂CH₂P(Ph)CH₂CH₂PPh₂)₂Br]Br,¹⁶ containing dangling arm phosphine oxide groups. In this work we have prepared Pd(II) and Pt(II) complexes of triphos and studied chelate ring-opening reactions induced by Au(I) with a view to obtaining mixed metal complexes. The X-ray crystal structure of [Pd(triphos)Cl]Cl, **1**, has been previously reported by

Housecroft *et al.*,¹⁷ and that of [Pt(triphos)Cl]Cl, **2**, is discussed in the present study and compared with **1** and the analogous Ni complexes.^{18,19} We report the X-ray crystal structure of the bimetallic complexes **3** and **4**, in which triphos acts as a bidentate chelating ligand, coordinating through the central and terminal phosphorus atoms,^{19,20} and have investigated reactions of potential biological importance including those with the nucleotide 5'-GMP and S-containing amino acids in aqueous media.

Experimental

Solvents were redistilled under nitrogen over CaCl₂ (acetone) and P₄O₁₀ (CHCl₃). Other reagents were of the highest commercial grade available and were used as received. Microanalyses were performed at the University of Santiago de Compostela and Department of Chemistry, University College London. Fast Atom Bombardment (FAB) spectra were obtained on a KRATOS MS 50 spectrometer using 3-nitrobenzyl alcohol as the matrix. Infrared spectra were recorded at ambient temperature as KBr pellets (4000–500 cm⁻¹) and Nujol mulls (500–100 cm⁻¹) on a Mattson Cygnus 100 spectrophotometer. The bands are reported as: vs = very strong, s = strong, m = medium, w = weak, and sh = shoulder. Conductivities were obtained at 25 °C from 10⁻³ M solutions in DMF on a WTW model LF-3 instrument. ³¹P{¹H} NMR spectra were recorded on either a Bruker AMX500 at 202.46 MHz, a Jeol GSX270 NMR at 109.25 MHz, or a Bruker DMX 500 spectrometer at 202 MHz. ¹⁹⁵Pt NMR were recorded on a Jeol GSX270 at 57.94 MHz. ¹H NMR spectra were recorded on a Bruker DMX 500 spectrometer at 500.13 MHz. Chemical shifts are reported in ppm relative to external 85% H₃PO₄ (³¹P), 1 M Na₂PtCl₆ (¹⁹⁵Pt) and sodium 3-(trimethylsilyl)propionate (¹H); δ = chemical shift in ppm; s = singlet, t = triplet,

d = doublet, dd = doublet of doublets, dt = doublet of triplets, m = multiplet, br = broad, J = coupling constant in Hz.

The pH values of the solutions were determined using a Corning 240 pH meter equipped with an Aldrich micro combination electrode, calibrated with Aldrich buffer solutions at pH 4, 7 and 10. For mixed solvents, the pH meter reading is given without correction.

Solutions of Au(I) were prepared by treating Au (0.25 g, 0.127 mmol) with 2.5 ml HCl (36%) and 1.5 ml HNO₃ (60%) on an oil bath (120 °C), followed by the addition of 2 × 2.5 ml HCl.²¹ It was then allowed to cool to room temperature. Water (10 ml) was then added, the solution was neutralised with CaCO₃, and the resultant suspension was filtered off. The clear final solution was reduced with 2,2'-thiodiethanol (1 ml) until the colour changed from yellow to colourless, to give Au(I) *in situ*.²² Alternatively, Au(I) was prepared directly by reduction of NaAuCl₄ with 2,2'-thiodiethanol.

Preparation of complexes

[Pd(triphos)Cl]Cl²³ **1**. A suspension of PdCl₂ (0.12 g, 0.67 mmol) and NaCl (0.08 g, 1.33 mmol) in H₂O (15 ml) was heated on a water bath (80 °C) until a clear solution was formed. This was allowed to cool to ambient temperature and triphos (0.4 g, 0.75 mmol) in CH₂Cl₂ (30 ml) was added dropwise. The resultant solution was stirred for 1 h at ambient temperature and solvent removed *in vacuo* to leave a white solid. The solid was filtered off, washed with water, dried *in vacuo* and recrystallized from CH₂Cl₂-n-hexane, to give colourless prisms. Yield 68%, mp >250 °C (Found: C, 57.01; H, 4.90. Calc. for C₃₄H₃₃P₃PdCl₂: C, 57.31; H, 5.16%). m/z (FAB) 675 ($M^+ - Cl$, 100%); 658 (ClPdC₃H₃P₃Ph₅, 27.7); 428 (ClPdC₃HP₃Ph₂³⁺, 32.1); 338 (ClPdC₂HP₃Ph₂²⁺, 33.5); 229 (PdCHPPH₂⁺, 27.6), 215 (PdPPH₂⁺, 13); 108 (PPh₂, 15.9%). IR $\nu_{\max}/\text{cm}^{-1}$ (PdCl) 318 vs. ³¹P{¹H} NMR (CDCl₃): δ 44.22 [2P, d, $J(P-P) = 9.4$ Hz, -PPh₂]; 109.34 (1P, t, P_bPh). λ (DMF): 91.48 $\Omega^{-1} \text{cm}^2 \text{mol}^{-1}$.

[Pt(triphos)Cl]Cl²³ **2**. A solution of triphos (0.80 g, 1.49 mmol) in CH₂Cl₂ (40 ml) was added dropwise to a solution of K₂PtCl₄ (0.58 g, 1.39 mmol) in H₂O (20 ml). The final solution was stirred for 1 h and solvent removed *in vacuo* to leave a white solid. The solid was filtered off, washed with water, dried *in vacuo* and recrystallized from CH₂Cl₂-n-hexane, to give colourless prisms. Yield: 70%, mp 200 °C (Found C, 50.79; H, 4.38. Calc. for C₃₄H₃₃P₃PtCl₂: C, 50.96; H, 4.12%). m/z (FAB) 764 ($M^+ - Cl$, 100%); 578 (PtC₄H₈P₃Ph₃³⁺, 25); 411 (PtP₂Ph₂, 11.6); 185 (PPh₂, 45.2%). IR $\nu_{\max}/\text{cm}^{-1}$ (PtCl) 320 vs. 314 sh. ³¹P{¹H} NMR (CDCl₃): δ 39.82 [2P, s, $J(P-Pt) = 2484$ Hz, -PPh₂]; 83.69 [1P, s, $J(P-Pt) = 3015$ Hz, P_bPh]. ¹⁹⁵Pt NMR (CDCl₃): δ -4858.3 [dt, $J(Pt-P) = 2484, 3015$ Hz]. λ (DMF): 82.87 $\Omega^{-1} \text{cm}^2 \text{mol}^{-1}$.

[PdAu(triphos)Cl₃] **3**. A solution of Au(I) (0.049 g of Au, 0.25 mmol), prepared as described above, was added dropwise to a solution of [Pd(triphos)Cl]Cl (0.18 g, 0.25 mmol) in ethanol-methanol (60 ml-10 ml). A white precipitate appeared immediately. After the volume was reduced, the resulting solid was filtered off, washed with water and dried. Yield: 51%, mp 141 °C (Found: C, 43.10; H, 3.50; P, 9.63; Cl, 11.31. Calc. for C₃₄H₃₃P₃PdAuCl₃: C, 43.19; H, 3.49; P, 9.84; Cl, 11.27%). m/z (FAB) 907 ($M^+ - Cl$, 92); 874 ($M^+ - 2Cl$, 26); 689 (ClAuPdC₄H₈P₂Ph₃²⁺, 97); 675 (ClAuPdC₃H₆P₂Ph₃²⁺, 77); 428 (PdC₂H₄P₂Ph₃²⁺, 30.5), 185 (PPh₂, 37.9%). IR $\nu_{\max}/\text{cm}^{-1}$ (AuCl) 317 vs. (PdCl) 290 sh. ³¹P{¹H} NMR (CDCl₃): δ 33.48 [1P, d, $J(P-P) = 63$ Hz, -PPh₂Au]; 65.47 [1P, d, $J(P-P) = 10$ Hz, -PPh₂Pd]; 72.96 (1P, dd, P_bPhPd). λ (DMF): 9.2 $\Omega^{-1} \text{cm}^2 \text{mol}^{-1}$.

[PtAu(triphos)Cl₃] **4**. To a solution of [Pt(triphos)Cl]Cl (0.2 g, 0.25 mmol) in ethanol (20 ml), a solution of Au(I) (0.05 g

of Au, 0.25 mmol), prepared as described above, was added dropwise. The white precipitate was filtered off, washed with water and dried. Yield: 60%, mp 159 °C (Found: C, 39.48; H, 3.19; P, 9.19; Cl, 10.70. Calc. for C₃₄H₃₃P₃PtAuCl₃: C, 39.50; H, 3.19; P, 9.00; Cl, 10.31%). m/z (FAB) 996 ($M^+ - Cl$, 6.2), 963 ($M^{2+} - 2Cl$, 4.5), 927 ($M^+ - 3Cl$, 6.8), 776 (AuPtC₄H₈P₃Ph₃³⁺, 13.9), 578 (PtC₄H₈P₃Ph₃²⁺, 9.6), 136 (C₂H₄PPh₂, 100%). IR $\nu_{\max}/\text{cm}^{-1}$ (AuCl) 325 sh. (PtCl) 293 vs. ³¹P{¹H} NMR (CDCl₃): δ 30.20 [1P, d, $J(P-P) = 61.7$ Hz, -PPh₂Au]; 41.23 [1P, s, $J(P-Pt) = 3590$ Hz, -PPh₂Pt]; 47.13 [1P, d, $J(P-Pt) = 3600$ Hz, P_bPhPt]. ¹⁹⁵Pt NMR (CDCl₃): δ -4592 [dd, $J(Pt-P) = 3600$ Hz]. λ (DMF): 6.2 $\Omega^{-1} \text{cm}^2 \text{mol}^{-1}$.

Titration of complex 1 with Au(I). A solution of Au(I) (0.0022 g of Au, 0.01 mmol) prepared as described previously, in MeOH (1 ml), was added dropwise to a solution of complex **1** (0.00787 g, 0.01 mmol) in CDCl₃ (2.5 ml). After 24 h a ³¹P-¹H NMR spectrum was recorded. This procedure was repeated after additions of two and three molar equivalents of Au(I).

Titration of complex 2 with Au(I). A solution of Au(I) (0.0022 g of Au, 0.01 mmol) in MeOH (1 ml) was added dropwise to a solution of complex **2** (0.00896 g, 0.01 mmol) in CDCl₃ (2.5 ml). ³¹P-¹H NMR spectra were recorded after 24 h. Further additions of two and three molar equivalents of Au(I) were made after the same time interval.

Reaction of [Pt(triphos)Cl]Cl, 2, with reduced glutathione (GSH). To a solution of [Pt(triphos)Cl]Cl (0.015 g, 0.02 mmol) in CD₃OD (0.4 ml), a solution of AgNO₃ (0.0064 g, 0.04 mmol) in D₂O (0.1 ml) was added. The precipitate was filtered off, and to the clear solution, a solution of GSH (0.0057 g, 0.02 mmol) in D₂O (0.1 ml) was added. The pH was adjusted to 7.88 and the ³¹P and ¹H NMR spectra were recorded.

Reaction of [Pt(triphos)(SG)]⁺, 5, with 5'-GMP in the presence of Au(I). To a solution of [Pt(triphos)Cl]Cl (0.015 g, 0.02 mmol) in CD₃OD (0.5 ml) a solution of AgNO₃ (0.0096 g, 0.06 mmol) in D₂O (0.1 ml) was added. After removing the precipitate, a solution of GSH (0.0057 g, 0.02 mmol) in D₂O (0.1 ml) was added and the pH adjusted to 7.35. Solutions of 5'-GMP (0.0076 g, 0.02 mmol) in D₂O (0.1 ml), AgNO₃ (0.0192 g, 0.11 mmol) in D₂O (0.1 ml) and [Au(thiodiglycol)Cl] (0.0037 g of Au, 0.02 mmol) in CD₃OD (0.2 ml), prepared as described earlier, were added to the clear solution. After removal of the precipitate (AgCl) the ³¹P and ¹H NMR spectra were recorded.

Reaction of [Pt(triphos)Cl]Cl, 2, with N-acetyl-L-cysteine. A solution of AgNO₃ (0.0064 g, 0.04 mmol) in D₂O (0.1 ml) was added to a solution of [Pt(triphos)Cl]Cl (0.015 g, 0.02 mmol) in CD₃OD (0.4 ml). The precipitate was filtered off, and a solution of N-acetyl-L-cysteine (0.0031 g, 0.02 mmol) in D₂O (0.1 ml) was added to the clear solution and pH was adjusted to 7.30. ³¹P and ¹H NMR spectra of the solution were recorded.

Reaction of [Pt(triphos)Cl]Cl, 2, with N-acetyl-L-methionine. To a solution of [Pt(triphos)Cl]Cl (0.015 g, 0.02 mmol) in CD₃OD (0.4 ml), a solution of AgNO₃ (0.0064 g, 0.04 mmol) in D₂O (0.1 ml) was added. After removing the precipitate, a solution of N-acetyl-L-methionine (0.0036 g, 0.02 mmol) in D₂O (0.1 ml) was added to the clear solution and pH was adjusted to 7.64. ³¹P and ¹H NMR spectra of the solution were recorded.

Reaction of [PtAu(triphos)Cl₃], 4, with GSH. 1:1 Molar ratio. To a solution of [PtAu(triphos)Cl₃] (0.020 g, 0.02 mmol) in DMF (0.25 ml) a solution of GSH (0.006 g, 0.02 mmol) in D₂O (0.5 ml) was added. A white precipitate was formed, which was filtered off and the ³¹P NMR spectrum of the solution was recorded. The pH of the solution was *ca.* 3.

Table 1 Summary of crystal parameters, data collection and refinement for the crystal structures⁶³

Complex	2	3	4
Empirical formula	C ₃₄ H ₃₃ Cl ₂ P ₃ Pt	C ₃₇ H ₃₆ AuCl ₁₂ P ₃ Pd	C ₃₇ H ₃₆ AuCl ₁₂ P ₃ Pt
Formula weight	800.50	1302.33	1391.11
<i>T</i> /K	293(2)	223(2)	150
$\lambda/\text{\AA}$	0.71073	1.54184	0.71073
Crystal size/mm	0.40 × 0.25 × 0.20	0.23 × 0.19 × 0.02	0.23 × 0.19 × 0.08
Colour/habit	Colourless/prisms	Colourless/plates	Colourless/plates
Crystal system	Monoclinic	Monoclinic	Monoclinic
Space group	<i>P2₁/n</i>	<i>P2₁/n</i>	<i>I2/a</i>
<i>a</i> /\AA	10.225(2)	14.0543(10)	23.077(7)
<i>b</i> /\AA	20.393(2)	15.6271(11)	15.842(11)
<i>c</i> /\AA	15.775(2)	22.714(2)	28.838(19)
$\alpha/^\circ$	—	—	—
$\beta/^\circ$	96.22(2)	104.724(5)	109.53(3)
$\gamma/^\circ$	—	—	—
<i>V</i> /\AA ³	3270.0(8)	4824(6)	9936
<i>Z</i>	4	4	8
Calculated density/Mg m ⁻³	1.626	1.793	1.86
Absorption coefficient/mm ⁻¹	4.624	15.915	6.56
<i>F</i> (000)	1576	2528	5312
θ range for data collection/ $^\circ$	2.60 to 26.30	3.47 to 60.01	2.5 to 22.5
Index ranges	0 ≤ <i>h</i> ≤ 12 −25 ≤ <i>k</i> ≤ 0 −19 ≤ <i>l</i> ≤ 19	15 ≤ <i>h</i> ≤ 15 −6 ≤ <i>k</i> ≤ 17 −5 ≤ <i>l</i> ≤ 25	−24 ≤ <i>h</i> ≤ 23 0 ≤ <i>k</i> ≤ 17 0 ≤ <i>l</i> ≤ 30
Reflections collected	7014	7778	7130
Independent reflections	6638 [<i>R</i> _{int} = 0.0248]	5997 [<i>R</i> _{int} = 0.0777]	5529 [<i>R</i> _{int} = 0.0826]
Absorption correction	Semi-empirical	Semi-empirical	Semi-empirical
Max. and min. transmission	0.977 and 0.794	0.182 and 0.719	0.175 and 0.283
Data/restraints/parameters	6638/0/372	5958/0/487	3150/28/212
Goodness of fit on <i>F</i> ²	1.025	1.045	1.18
Final <i>R</i> indices ^{a,b}	<i>R</i> ₁ = 0.0366, <i>wR</i> ₂ = 0.1061	<i>R</i> ₁ = 0.0485, <i>wR</i> ₂ = 0.1276	<i>R</i> ₁ = 0.1086, <i>wR</i> ₂ = 0.0963
Largest diff. peak and hole (e [−] \AA ^{−3})	1.190 and −0.646	0.765 and −0.835	4.55 and −2.83

^a [*I* > 2 σ (*I*)] for **2**, [*I* > 4 σ (*I*)] for **3** and **4**. ^b *wR*₂ = [$\sum w(F_o^2 - F_c^2)^2 / \sum w(F_o^2)^2$]^{1/2}.

1:2 Molar ratio. A solution of GSH (0.09 g, 0.03 mmol) in D₂O (0.5 ml) was added to a solution of [PtAu(triphos)Cl₃] (0.015 g, 0.015 mmol) in DMF (0.4 ml). A white precipitate was formed, which was filtered off. The pH of the solution was adjusted to 7.53 and the ³¹P NMR spectrum of the solution recorded.

Reaction of [PtAu(triphos)Cl₃] with *N*-acetyl-L-cysteine. 1:1 Molar ratio. To a solution of [PtAu(triphos)Cl₃] (0.02 g, 0.02 mmol) in DMF (0.25 ml), a solution of *N*-acetyl-L-cysteine (0.0032 g, 0.02 mmol) in D₂O (0.5 ml) was added. A white precipitate immediately formed, which was filtered off and the ³¹P NMR spectrum of the solution was recorded. The pH of the solution was ca. 3.

1:2 Molar ratio. A solution of *N*-acetyl-L-cysteine (0.0047 g, 0.03 mmol) in D₂O (0.5 ml) was added to a solution of [PtAu(triphos)Cl₃] (0.015 g, 0.015 mmol) in DMF (0.4 ml). A white precipitate was formed, this was filtered off, the pH adjusted to 7.21 and the ³¹P NMR spectrum of the solution recorded.

Crystallography

Table 1 summarises the crystal data, data collection, structural solution and refinement parameters for complexes **2–4**. A colourless prismatic crystal of **2** was mounted on glass fiber and used for data collection. Cell constants and an orientation matrix for data collection were obtained by least-squares refinement of diffraction data from 25 reflections in the range 10.37° < θ < 17.98° in an Enraf Nonius MACH3 automatic diffractometer.²⁴ Data were collected at 293 K using Mo-K α radiation and the ω scan technique and corrected for Lorentz and polarization effects.²⁵ A semi-empirical absorption correction was made (Ψ -scan).²⁶

The structures were solved by direct-methods²⁷ which revealed the position of all non-hydrogen atoms, and refined on *F*² by a full-matrix least-squares procedure using anisotropic

displacement parameters.²⁸ The chloride ion is disordered: occupancies of 0.717(5) and 0.283(5) for Cl(21) and Cl(22), respectively. The hydrogen atoms were located in their calculated positions (C–H = 0.93–0.97 \AA). The located H atoms were refined isotropically, whereas the calculated H atoms were refined using a riding model. A secondary extinction correction was applied.²⁸ Relatively large positive peaks were found in the final difference Fourier map, but these were all error peaks located near the Pt and Cl atoms. Atomic scattering factors were taken from *International Tables for X-Ray Crystallography*.²⁹ For molecular graphics the programs PLATON,²⁶ SCHAKAL92³⁰ and ZORTEP³¹ were used.

The X-ray data for **3** and **4** were collected on Stoe Stadi4 four-circle diffractometers equipped with an Oxford Cryo-systems variable temperature device.³² Complex **3** crystallised as very thin plates and Cu-K α radiation was used for data collection because it is more intense than Mo-K α radiation (which might have been preferred on grounds of minimising absorption effects). Data were collected with $\omega - \theta$ scans using on-line profile fitting.³³ The structure was solved by Patterson methods and completed by iterative cycles of least-squares refinement and ΔF -syntheses.³⁴ H-atoms were placed in calculated positions and treated as riding on the atoms to which they are attached. Anisotropic displacement parameters were refined for all non-H atoms. One of the three molecules of HCCl₃ of crystallization exhibits large anisotropic displacement parameters (*adp*'s); attempts to model this over two discrete orientations led to no improvement in the data-fitting, and so the disorder was treated as being essentially modelled by the *adp*'s.

Crystals of **4** were of a much lower quality than those of **3**; this naturally lowered the precision of the crystal structure, which can be taken to establish chemical connectivity, but which cannot be further interpreted. Data were collected using Mo-K α radiation and ω -scans. The structure was solved by Patterson methods and completed by iterative cycles of least-

Table 2 ^{31}P and ^{195}Pt NMR (CDCl_3): chemical shifts (ppm), multiplicity and coupling constants (Hz), $\Delta\delta$ = coordination chemical shift for complexes **1** and **2** (a) **3** and **4**, (b). For atom labelling see Scheme 1

(a)	1		2	
	δ or J	$\Delta\delta$	δ or J	$\Delta\delta$
$\delta(\text{P}_a)$	44.22 (d)	58.6	39.82 (s)	54.2
$\delta(\text{P}_b)$	109.34 (t)	127.6	83.69 (s)	101.9
$\delta(\text{Pt})$	—	—	-4858 (dt)	—
$J(\text{P}_a-\text{P}_b)$	9.4	—	—	—
$J(\text{P}_a-\text{Pt})$	—	—	2484	—
$J(\text{P}_b-\text{Pt})$	—	—	3015	—
(b)	3		4	
	δ or J	$\Delta\delta$	δ or J	$\Delta\delta$
$\delta(\text{P}_c)$	65.47 (d)	79.8	41.23 (s)	54.9
$\delta(\text{P}_d)$	72.96 (dd)	90.2	47.13 (d)	65.1
$\delta(\text{P}_e)$	33.48 (d)	47.9	30.20 (d)	44.9
$\delta(\text{Pt})$	—	—	-4592 (dd)	—
$J(\text{P}_c-\text{P}_d)$	10.0	—	—	—
$J(\text{P}_d-\text{P}_e)$	63.0	—	61.7	—
$J(\text{P}_c-\text{Pt})$	—	—	3590	—
$J(\text{P}_d-\text{Pt})$	—	—	3600	—

squares refinement and ΔF -syntheses.³⁵ Residual absorption errors were treated using DIFABS³⁶ (max. and min. corrections 1.358 and 0.679, respectively). Only the Pt, P, Au and Cl atoms were refined anisotropically; the phenyl groups were treated as rigid rotating groups and atoms within the same phenyl group were given equal isotropic thermal parameters. Similarity restraints were applied to the lengths of C2–C3 and C5–C6 and to the geometries of the solvent molecules. C2, C3, C5 and C6 and the C-atoms of the solvent molecules were respectively assigned two common isotropic thermal parameters. H-atoms were placed in calculated positions.

CCDC reference number 186/1535.

See <http://www.rsc.org/suppdata/dt/1999/2861/> for crystallographic files in .cif format.

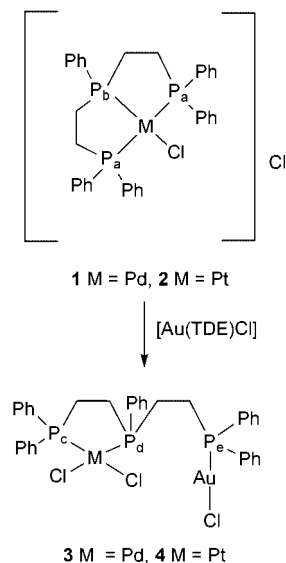
Results and discussion

Preparations

Complex **1** was prepared using a variation of a literature method²³ which gave a higher yield than previously reported.³⁷ The route involved reaction of triphos and PdCl_2 in $\text{H}_2\text{O}-\text{CH}_2\text{Cl}_2$ (1:2) at ambient temperature and complex **1** was purified by recrystallization from CH_2Cl_2 -n-hexane (1:2), giving a final yield of 68%. The product was a colourless, crystalline solid, stable in air and towards moisture. The complex showed a high thermal stability with a melting point over 250 °C, and was fully characterised by microanalysis, ^{31}P NMR, and IR spectroscopies and FAB MS.

Complex **2** was prepared from triphos and K_2PtCl_4 , using the same procedure and was recrystallised from CH_2Cl_2 -n-hexane giving a colourless crystalline solid in 70% yield. This compound was also thermally stable with a mp of 200 °C. It was fully characterised by the same methods as complex **1**, and in addition the ^{195}Pt NMR spectrum was recorded. The NMR data are given in Table 2. Crystals suitable for X-ray crystallography were obtained from CH_2Cl_2 -n-hexane (1:2) and its structure was determined.

Solutions of Au(I) were prepared by the reduction of either HAuCl_4 or NaAuCl_4 with thiodiglycol²² and is believed to be present as $[\text{Au}(\text{thiodiglycol})\text{Cl}]$.³⁸ On reacting complexes **1** and **2** with 1 molar equivalent of Au(I) solution, the bimetallic complexes **3** and **4**, respectively, were obtained *via* ring-opening reactions (Scheme 1). These novel complexes were obtained in yields of 62% and 69%, respectively. They were colourless



Scheme 1 Ring-opening reactions of $[\text{M}(\text{triphos})\text{Cl}]\text{Cl}$ complexes, induced by $[\text{Au}(\text{TDE})\text{Cl}]$ (TDE = thiodiglycol).

crystalline solids and stable towards air and moisture. Both complexes melted without decomposition at 141 °C and 159 °C respectively. Crystals of these complexes suitable for X-ray crystallography were obtained from CDCl_3 solutions, and their structures were determined (see Crystallographic section). Complexes **3** and **4** were also prepared by the addition of a solution of $[\text{Au}(\text{triphos})\text{Cl}]$ in acetone to a suspension of MCl_2 ($\text{M} = \text{Pd}$ for **3** and $\text{M} = \text{Pt}$ for **4**) in the same solvent.

Mass spectra

FAB MS spectra for complexes **1** and **2** showed a base peak corresponding to the fragment $[\text{M}^+ - \text{Cl}]$ (675 Pd; 764 Pt); however, the pattern of fragmentation was different in each case. The loss of chlorine in the first step of fragmentation is typical of platinum and palladium dichloro complexes.³⁹ For $[\text{PdAu}(\text{triphos})\text{Cl}_3]$ the peak at 909 (92%) corresponds to $[\text{M}^+ - \text{Cl}]$. The loss of P–Ph₂ leads to the most abundant peak (97%) at m/z , 689. $[\text{PtAu}(\text{triphos})\text{Cl}_3]$ also lost chlorine to give $[\text{M}^+ - \text{Cl}]$ at m/z 996.

Infrared spectra

The far infrared spectra (500–100 cm^{-1}) for complexes **1** and **2** showed bands assignable, in agreement with the literature,²³ to the following bond vibrations: $\nu(\text{Pd}-\text{Cl}) = 318 \text{ cm}^{-1}$; $\nu(\text{Pt}-\text{Cl}) = 320, 314 \text{ cm}^{-1}$; $\nu(\text{Pd}-\text{P}) = 366, 353, 345 \text{ cm}^{-1}$; $\nu(\text{Pt}-\text{P}) = 372, 356, 349 \text{ cm}^{-1}$. In the bimetallic complexes **3** and **4**, $\nu(\text{M}-\text{Cl})$ (290 cm^{-1} and 293 cm^{-1} , respectively) are at lower wave numbers compared to **1** and **2**, consistent with relatively longer M–Cl distances for the above complexes. The Au–Cl stretch appears as a very strong band at 316 cm^{-1} for **3**, and as a shoulder at 325 cm^{-1} for **4**.

Conductivities

The molar conductivities for complexes **1** and **2** in 10^{-3} M DMF solutions (91.48 and 82.87 $\Omega^{-1} \text{ cm}^2 \text{ mol}^{-1}$, respectively) are indicative of 1:1 electrolytes.⁴⁰ Complexes **3** and **4** are neutral and do not conduct in DMF, as expected.

NMR spectra

The ^{31}P - $\{^1\text{H}\}$ and ^{195}Pt NMR data for complexes **1–4** are given in Table 2. The ^{31}P peak for **1** at 109.34 ppm can be assigned to the central phosphorus (P_b) and that at 44.22 ppm to the terminal phosphorus (P_a), on the basis of multiplicity, integration (1:2) and in comparison with complex **2** (*vide infra*). The ^{31}P NMR spectrum for complex **2** showed peaks at 83.69

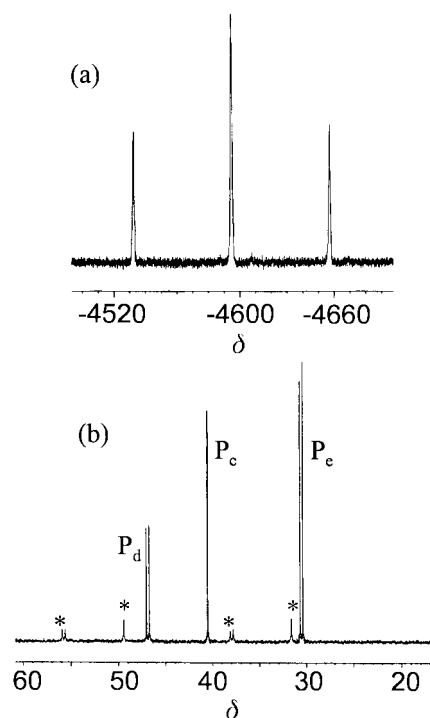


Fig. 1 NMR spectra for a CDCl_3 solution of $[\text{PtAu}(\text{triphos})\text{Cl}]_3$, **4**, at 20 °C. (a) ^{195}Pt , (b) ^{31}P . For ^{31}P NMR spectrum peaks labelled as P_c (terminal P bound to platinum), P_d (central P) and P_e (terminal P bound to gold). In (b) ^{195}Pt satellites are indicated by *. For atom labelling see Scheme 1.

ppm(s) and 39.82 ppm(s), with $^1J(\text{P-Pt})$ values of 3015 and 2484 Hz, values typical of P *trans* to Cl (P_b) and P *trans* to P (P_a), respectively.^{41,42} For **2**, P–P coupling was not observed. The ^{31}P NMR peaks for triphos in CDCl_3 [–18.2 (t) and –14.5 (d) ppm] undergo large downfield shifts upon complexation (see Table 2). Such lowfield shifts ($\Delta\delta$) have been found for related chelated phosphines. The magnitude of $\Delta\delta$ for chelated phosphines is dependent on the size and number of chelate rings containing the phosphorus atom. For the central phosphorus (P_b) in complexes **1** and **2**, $\Delta\delta$ values are *ca.* 128 and 102 ppm, respectively, very large compared to those of the terminal phosphorus (P_a): *ca.* 60 and 55 ppm for these complexes. The large difference in $\Delta\delta$ values for the central and terminal phosphorus, is due to the central phosphorus (P_b) being part of two five-membered chelate rings. For complexes **3** and **4**, $\Delta\delta$ for phosphorus atoms chelating Pd and Pt (P_c and P_d) is larger than for phosphorus atoms bound to gold (P_e) as expected (Table 2). It is also observed that the ^{31}P peak for the central phosphorus atom (P_b) of the parent complexes **1** and **2** is shifted to high field (by *ca.* 40 ppm) upon ring-opening.

The ^{31}P NMR spectrum for complex **3** showed three peaks at 33.48 (d), 65.47 (d) and 72.96 (dd) ppm. The $^2J(\text{P-P})$ and $^3J(\text{P-P})$ values were 10 and 63 Hz, respectively, corresponding to coupling of the central P_d with the terminal P bound to Pd (P_c) and the terminal P bound to Au (P_e). These values are in agreement with those reported for related compounds.⁴⁴

For complex **4**, the ^{31}P NMR spectrum had peaks at 30.20 (d), 41.23 (s), 47.13 (d) ppm, with $^1J(\text{P-Pt})$ values of 3590 and 3600 Hz and $^3J(\text{P-P})$ values of 61.7 Hz. These P–Pt coupling constants are indicative of P *trans* to Cl.^{41,42} Thus from the above data, the latter two peaks can be assigned to P bound to Pt (P_c and P_d respectively), and the former peak to the P bound to Au (P_e) as it does not display Pt satellites.

The ^{195}Pt NMR spectrum of **2** was a doublet of triplets (–4858 ppm) with $^1J(\text{Pt-P})$ values of 3015 and 2484 Hz. These coupling constants are typical of P *trans* to Cl and P *trans* to P, respectively.^{41,42,45} The ^{195}Pt NMR spectrum of **4**, Fig. 1(a), is expected to be a doublet of doublets, because Pt is bound to

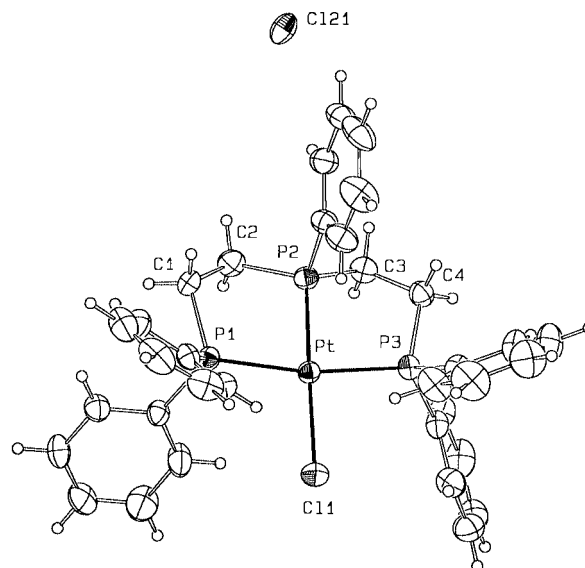


Fig. 2 ORTEP view of $[\text{Pt}(\text{triphos})\text{Cl}]\text{Cl}$, **2**.

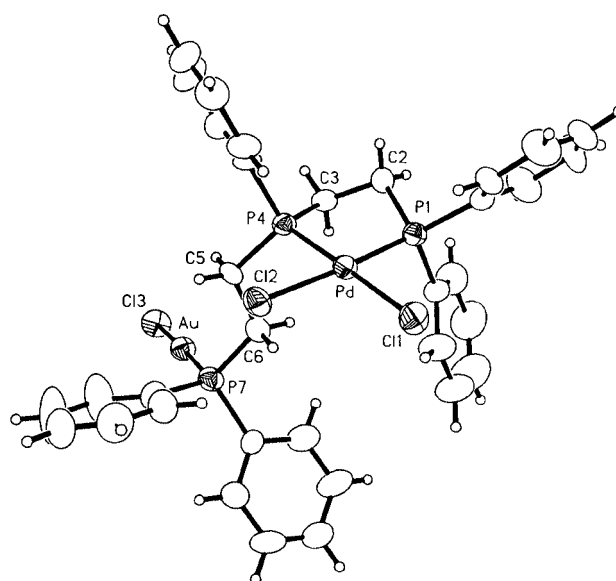


Fig. 3 ORTEP view of $[\text{PdAu}(\text{triphos})\text{Cl}]_3$, **3**.

two inequivalent phosphorus atoms. However, they appear to have the same coupling constant [$J(\text{Pt-P}) = 3600$ Hz], with the result that the resonance appeared as a triplet. The value of this coupling constant is consistent with P *trans* to Cl.^{46,47} Thus the ^{195}Pt NMR data are within the expected range for this type of complexes.

Crystallography

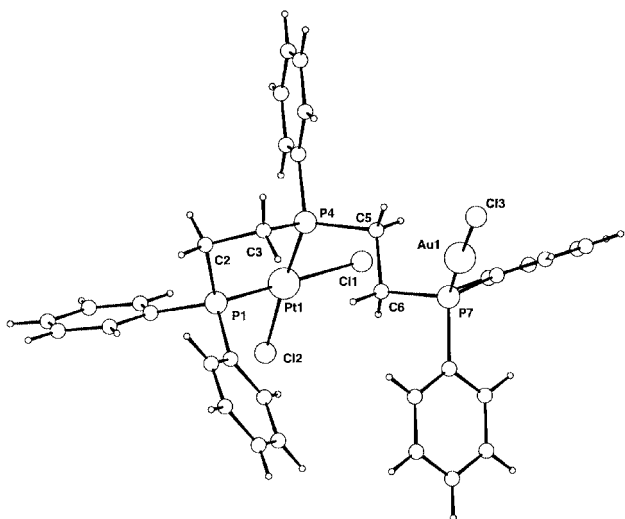
ORTEP⁶³ diagrams with the numbering schemes for complexes **2–4** are shown in Fig. 2–4. Summaries of crystal parameters, data collection and refinement for the crystal structures are given in Table 1, and selected bond lengths and angles are listed in Table 3.

The molecular structure and numbering scheme for complex **2** are shown in Fig. 2. The complex has a distorted square-planar geometry for platinum. The Pt–P bond lengths of 2.315(2) (P1), 2.207(2) (P2) and 2.312(2) (P3) Å are in the expected range. The Pt–P(2) bond distance is found to be shorter than the Pt–P_{terminal} due to the double chelate effect. The P–Pt–Cl angles, 97.50(7), 176.52(7), 92.94(7)° and the P–Pt–P, 84.69(7), 169.54(6) and 84.92(7)°, show the distorted square-planar environment at platinum. The distortion is higher for Ni complexes (X = Cl, I).⁴⁸ In complexes **1** and **2** the chloride

Table 3 Selected distances (Å), angles (°) and dihedral angles (°) for complexes 1–4

	1 ^a	2	3	4
	[Pd(triphos)Cl]Cl	[Pt(triphos)Cl]Cl	[PdAu(triphos)Cl ₃]	[PtAu(triphos)Cl ₃]
P–M	2.220(2) 2.328(2) 2.344(2)	2.207(2) 2.312(2) 2.315(2)	2.233(3) 2.234(3)	2.22(1) 2.23(1)
P–Au	—	—	2.228(3)	2.20(1)
M–Cl	2.355(2)	2.349(2)	2.351(3) 2.371(2)	2.354(8) 2.39(1)
Au–Cl	—	—	2.288(3)	2.296(9)
P–M–P	83.80(1) 84.10(1) 167.80(1)	84.69(7) 84.92(7) 169.54(6)	85.49(9)	86.4(3)
P–M–Cl	93.60(1) 98.50(1) 176.40(1)	92.94(7) 97.50(7) 176.52(7)	87.56(9) 93.64(10) 172.71(9) 177.74(11)	89.3(3) 93.7(3) 174.5(3) 176.1(3)
Cl–M–Cl	—	—	93.22(9)	90.4(3)
P–Au–Cl	—	—	177.73(10)	177.2(3)
Au···Au	—	—	4.155(7)	3.995(4)
I–II ^b	73.15	72.73	67.46	63.51
III–C ^b	83.20	83.24	69.15	70.99
IV–V ^b	88.08	88.16	72.77	80.11

^a See ref. 17. ^b Angles between planes defined as: I (C11–C16) (1–4), II (C21–C26) (1–2), II (C11'–C16') (3) and II (C111–C161) (4), III (C31–C36) (1–2) and III (C41–C46) (3–4) and IV (C71–C76) (3–4), V (C51–C56) (1–2), V (C71'–C76') (3) and V (C711–C761) (4), C [Pd–P(1)–P(2)–P(3)–Cl(1)] (1), C [Pd–P(1)–P(2)–P(3)–Cl(1)] (2), C [Pd–Cl(1)–Cl(2)–P(1)–P(4)] (3) and C [Pt–P(1)–P(4)–C(2)–C(3)] (4).

**Fig. 4** ORTEP view of [PtAu(triphos)Cl₃] 4.

ion is disordered over two positions, and for platinum complex 2 the occupancies are 0.717 and 0.283.

As found for [Ni(triphos)X]⁺ (X = Cl, I) complexes,⁴⁸ the phenyl substituents are slightly disordered. Labelling the phenyl ring planes as I (C11–C16), II (C21–C26) [substituents on P(1)], III (C31–C36) [substituent on P(2)], IV (C41–C46), V (C51–C56) [substituents on P(3)], and the best metal coordination plane, C [Pt–P(1)–P(2)–P(3)–Cl(1)], it is found that they are oriented differently. The Pt atom does not depart significantly from C (0.014 Å) compared to the mean value of 0.036 Å for atoms defining the plane. The dihedral angles between best planes C–I, I–II, II–III, III–IV and IV–V are 51.89, 72.73, 65.80, 33.16 and 88.16° respectively. The steric effects around P(1) and P(3) atoms result in similar I–II and IV–V dihedral angles (72.73° and 88.16°) and the less crowded environment of P(2) results in a phenyl plane, III, nearly perpendicular to the best major plane C. The coordination effect of Ni on triphos gives rise to a I–II dihedral angle *ca.* 30° higher than for Pt or Pd and the substitution of Cl by I does not affect this significantly.⁴⁸ This suggests that the dynamics of the structures is related to the steric effects near the phenyl substituents and to inter- and intra-cationic interactions in the crystal lattice.

Thus, for complex 2, the phenyl substituents of P(1) lie in the space between phenyl rings of P(3) in the adjacent molecule. Phenyl rings for complex 1 show a less hindered cell with different packing between adjacent molecules.¹⁷ The inter-cationic M···Cl contact is 2.884(9) Å with C–H···Cl angle 117.50(2)°. H···Cl intra-cationic interactions are 2.849(9), 2.932(9) and 2.964(8) Å with calculated C–H···Cl angles 129.8(2), 136.0(2) and 145.4(2)° respectively. Similar contacts are found for complex 1.⁴⁹ These contacts fulfil the H···A distance and angular criteria for weak H-bonds (greater than the sum of the individual radii, *ca.* 3.0 Å).⁵⁰ The large Pt···Pt distance (*ca.* 10 Å) shows that metal–metal interactions are not present.⁵¹

The molecular structures and numbering schemes of complexes 3 and 4 are shown in Fig. 3 and 4. Selected bond distances and angles are given in Table 3. The structures 3 and 4 show that one of the chelate rings has opened and triphos coordinates to M in a bidentate mode, the chelate ring being similar to that generated by dppe (dppe = Ph₂PCH₂CH₂PPh₂). The free arm of the phosphine ligand in the absence of other acceptors can undergo oxidation and form four- and five-coordinate complexes.¹⁶ But in the presence of Au(I) linear coordination P–Au–Cl is obtained.⁵² The ring-opening reaction results in a chiral central phosphorus, with both enantiomers being present in the unit cell.

The Au–Cl bond length for complex 3 is 2.288(3) Å, similar to the literature value of 2.301(43) Å.⁵³ The complex shows two different Pd–Cl distances which is consistent with the two stretching bands found in the infrared. The Pd–Cl bond length 2.371(2) Å is longer than found in 1,¹⁷ as also predicted by far infrared spectra. On the other hand, Au–Cl distances are shorter than Pd–Cl which is in agreement with $\nu(\text{Au–Cl})$ being at higher wavenumber than $\nu(\text{Pd–Cl})$. The Pd–P(1) bond length for complex 3 is shorter than for 1, whereas Pd–P(4) is longer than Pd–P(2) of 1. The Pd–P_{central} bond distance increases as a consequence of the ring-opening. P–Pd–Cl angles confirm square-planar environment at Pd, and the P–Au–Cl angle is in agreement with linear coordination [177.73(10) Å].

Complex 4 has a similar structure to complex 3, with a square-planar environment around platinum and linear coordination for gold, but as the crystal structure has low precision, bond distances and angles cannot be discussed further.

The dihedral angles (Table 3) obtained from the planes: I (C11–C16), II (C11'–C16') [substituents on P(1) for complex 3]

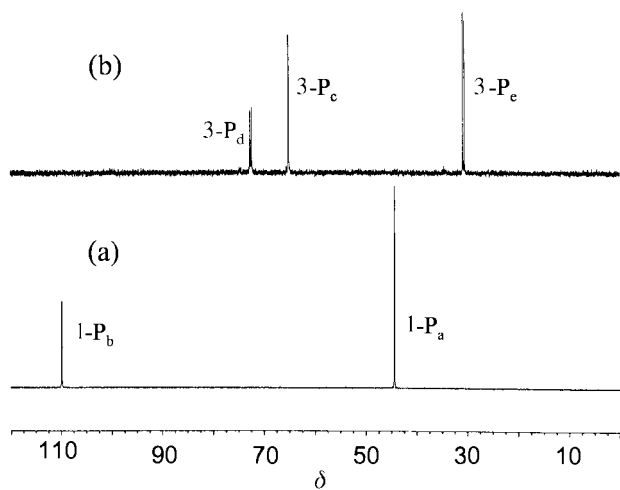


Fig. 5 ^{31}P NMR spectra of (a) complex **1** and (b) after addition of 1 mol. eq. of Au(I) affording complex **3** ($\text{CDCl}_3\text{-CD}_3\text{OD}$). Assignments: P_a (terminal P in complex **1**), P_b (central P in complex **1**), P_c (terminal P bound to palladium in complex **3**), P_d (central P in complex **3**) and P_e (terminal P bound to gold in complex **3**).

and I (C11–C16), II (C111–C161) [substituents on P(1) for complex **4**], III (C41–C46) [substituents on P(4) for complex **3** and **4**], IV (C71–C76), V (C71'–C76') [substituents on P(7) for complex **3**] and IV (C71–76), V (C711–C761) [substituents on P(7) for complex **4**] and the metal coordination planes C [Pd–Cl(1)–Cl(2)–P(1)–P(4)] complex **3** and [Pt–P(1)–P(4)–C(2)–C(3)] complex **4**, show that phenyl ring planes of terminal phosphorus form smaller angles (by *ca.* 6°) than complexes **1** and **2**. The phenyl ring plane of the central phosphorus forms angles of 69.15° (**3**) with plane C, a significant deviation from perpendicularity. The Pd atom is -0.035 \AA from C and this deviation is higher compared to the mean value of $+0.009 \text{ \AA}$ for atoms defining the plane.

Titration

The reaction of [Pd(triphos)Cl]Cl, **1** in $\text{CDCl}_3\text{-CD}_3\text{OD}$ solution with 1, 2 and 3 molar equivalents of Au(I) was followed by $^{31}\text{P}\text{-}\{^1\text{H}\}$ NMR spectroscopy. The disappearance of signals due to complex **1** and appearance of three new peaks at 30.69 (d), 65.19 (d) and 72.59 (dd) ppm (Fig. 5) corresponding to the phosphorus bound to gold (P_e), terminal phosphorus bound to palladium (P_c) and central phosphorus (P_d) respectively, show the opening of one of the chelate rings upon the addition of 1 molar equivalent of Au(I). These results indicate that [Pd–Au(triphos)Cl]₃, **3** is formed. Addition of 2 and 3 molar equivalents of Au(I) did not bring about any further changes.

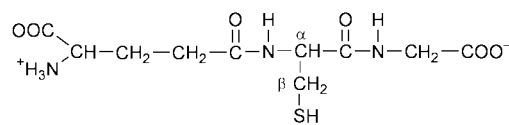
Titration of [Pt(triphos)Cl]Cl, **2** with 1 molar equivalent of Au(I), under the same conditions, as described for **1**, afforded a mixture of unreacted complex **2** together with the expected bimetallic complex **4**, and here again the ring-opening reaction was observed. The ability of Au(I) to ring open a triphos chelate may be due to the strong affinity of Au(I) for phosphorus together with chelate ring strain and the high *trans* effect of phosphorus.

The presence of relatively labile ligands in the attacking complex at Au(I) [Au(thiodiglycol)Cl] is important for inducing ring-opening since neither Me_3PAuCl nor Ph_3PAuCl reacted with complex **2** in CDCl_3 or DMF.

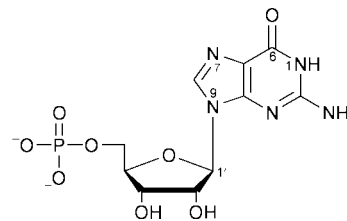
The oxidation of the bimetallic complex **4** to Au(III) with different oxidising agents (PCl_5 , Cl_2) in different solvents (CH_3CN , CH_2Cl_2) was attempted. However, no oxidation was observed when reactions were monitored by ^{31}P NMR. Electrochemical oxidation was also attempted in CH_2Cl_2 solutions, using TBAF_4 as electrolyte, but no peaks were observed in the cyclic voltammogram, showing that oxidation is not readily achieved.

Reactions with biologically relevant molecules

Reaction of [Pt(triphos)Cl]Cl, **2, with reduced glutathione (GSH).** The ^{31}P NMR spectrum of a solution containing complex **2** and GSH in 1 : 1 molar ratio at *ca.* pH 7.88, in $\text{CD}_3\text{OD-D}_2\text{O}$ (4 : 1), showed no new peaks. However after addition of



Glutathione (GSH)



5'-guanosine monophosphate (5'-GMP)

AgNO_3 and subsequent removal of the precipitate (AgCl), the ^{31}P spectrum showed peaks at 90.84 and 45.66 ppm assignable to P_b and P_a respectively, which are shifted to low field relative to unreacted complex **2**. The corresponding coupling constants were $J(\text{P}_a\text{-Pt}) = 2507 \text{ Hz}$, in the range of P *trans* to $\text{P}^{41,42}$ and $J(\text{P}_b\text{-Pt}) = 2443 \text{ Hz}$. The latter is within the lower range for P *trans* to S.⁵⁴ In the ^1H NMR spectrum, the $\beta\text{-CH}_2$ peak of the cysteine moiety was broadened and shifted by *ca.* 0.2 ppm to low field suggesting coordination through the S atom, as observed previously.⁵⁵ The ^1H and ^{31}P NMR spectra are consistent with the formation of [Pt(triphos)(GS)]⁺, **5**, where Pt(II) is bound to the sulfur atom of the cysteine residue. Formation of this adduct increases the aqueous solubility of triphos complexes, which may be biologically useful. Similar effects on the solubility of Pd(II) diphosphino and phosphinoarsino complexes upon reaction with GSH have been observed.⁵⁶

Reaction of [Pt(triphos)(GS)]⁺, **5, with 5'-GMP in the presence of Au(I).** Reaction of [Pt(triphos)Cl]Cl, **2** with GSH in 1 : 1 molar ratio at *ca.* pH 7.35 was carried out as described above, and formation of the [Pt(triphos)(GS)]⁺, **5**, was confirmed by ^{31}P and ^1H NMR (see above). 5'-GMP (1 molar equivalent) was added and ^{31}P and ^1H NMR were immediately recorded. The ^1H NMR spectrum showed the presence of free nucleotide in solution, but no peaks due to [Pt(triphos)(5'-GMP)] were present. The ^{31}P NMR spectrum showed broadening of the resonance assigned to P_b , a sharp peak assigned to P_a for complex **5** and one single peak in the phosphate region assignable to the phosphate group of the free nucleotide. Both spectra indicated that 5'-GMP did not displace glutathione from [Pt(triphos)(GS)]⁺, **5**.

The reaction of AgNO_3 with [Pt(triphos)(GS)]⁺, **5** was expected to result in the formation of a Ag–GS complex, as Ag(I) has high affinity for sulfur-containing amino acids,⁵⁷ and the resulting [Pt(triphos)(ONO₂)]NO₃ to react readily with 5'-GMP. Thus in order to facilitate the reaction of complex **5** with 5'-GMP excess AgNO_3 was added to the reaction mixture and the ^1H and ^{31}P NMR spectra recorded. However, these were found to be identical to those recorded earlier in the absence of AgNO_3 . This indicates that Ag(I) does not displace bound glutathione from [Pt(triphos)(GS)]⁺, **5**.

When [Au(thiodiglycol)Cl] (1 molar equivalent in CD_3OD) was added to a solution of complex **5**, [Pt(triphos)(GS)]⁺, prepared as above, together with 5'-GMP (1 molar equivalent in D_2O) and the ^{31}P and ^1H NMR spectra of the solution recorded, the spectra showed the formation of complex **2**,

Table 4 ^{31}P chemical shifts (ppm), multiplicity, coupling constants (Hz) and assignments for reactions of complexes **2** and **4** with biologically relevant molecules (1 : 1 molar ratio, except where stated)

Reactants	pH	P_a^d	$J(P_a\text{-Pt})$	P_b^d	$J(P_b\text{-Pt})$	Assignment
2 + GSH ^a	7.88	45.66 (s)	2507	90.84 (s)	2443	5
5 + 5'-GMP ^a	7.35	50.24 (s)	2419	80.48 (s)	2989	6a
		48.01 (s)	2431	77.81 (s)	—	6b
2 + <i>N</i> -acetyl-L-cysteine ^a	7.30	46.83 (s)	2518	92.05 (s)	2407	7
2 + <i>N</i> -acetyl-L-methionine ^a	7.64	47.13 (s)	2568	77.25 (s)	3157	8
		48.36 (s)	—	95.57 (s)	2739	
				94.83 (s)	2732	
4 + GSH ^b	3.0	42.99 (s)	2442	88.05 (s)	3099	2
4 + GSH ^{b,c}	7.53	45.45 (s)	2559	90.60 (s)	2319	5
4 + <i>N</i> -acetyl-L-cysteine ^b	3.0	42.93 (s)	2444	88.06 (s)	3095	2
4 + <i>N</i> -acetyl-L-cysteine ^{b,c}	7.21	45.12 (s)	2569	90.96 (s)	2292	7

^a CD₃OD–D₂O (2 : 1). ^b DMF–D₂O (4 : 1). ^c Molar ratio of reactants (1 : 2). ^d s = Singlet.

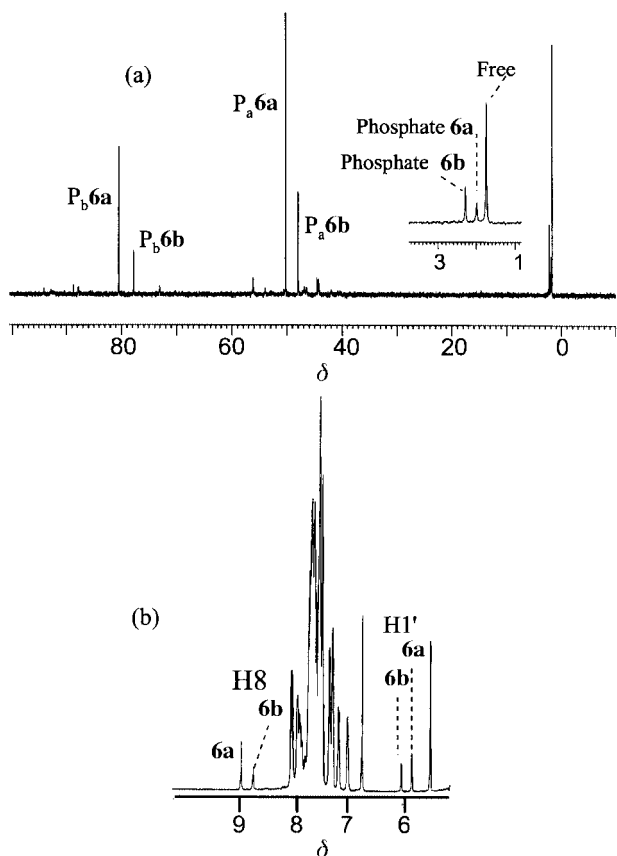


Fig. 6 (a) ^{31}P and (b) ^1H NMR spectra from the reaction of $[\text{Pt}(\text{triphos})(\text{GS})]^+$ **5** with 1 mol equivalent 5'-GMP in the presence of an excess of AgNO_3 and 1 mol equivalent $\text{Au}(\text{i})$. There are two isomeric products **6a** and **6b**. Peaks labelled P_a and P_b are assigned to the terminal and central phosphorus atoms, respectively, of the triphos ligand, and phosphate to the 5'-phosphate of the 5'-GMP ligand.

$[\text{Pt}(\text{triphos})\text{Cl}]\text{Cl}$ and no reaction with the nucleotide. This is probably as a result of the high affinity of $\text{Au}(\text{i})$ for thiolate sulfur and the presence of Cl^- in the reaction mixture which stabilises complex **2**. Thus in order to achieve nucleotide binding it was necessary to add AgNO_3 to remove the chloride present in the reaction mixture. The ^{31}P and ^1H NMR spectra of the solution of complex **5**, $[\text{Pt}(\text{triphos})(\text{GS})]^+$, 5'-GMP (1 molar equivalent), an excess of AgNO_3 and 1 molar equivalent of $\text{Au}(\text{i})$ showed two new sets of signals indicating the formation of two different 5'-GMP adducts, $[\text{Pt}(\text{triphos})(5'\text{-GMP-N7})]$ (**6a** and **6b**, Fig. 6). In the region of 81–77 ppm: two resonances at 80.48 ppm, $J(\text{P-Pt}) = 2989$ Hz and 77.81 ppm appeared and in the region of 50–45 ppm two peaks were observed at 50.24 and 48.01 ppm, with the corresponding coupling constants of $J(\text{P-Pt}) = 2419$ and 2431 Hz, respectively.

The former peaks were assigned to P_b and the latter to P_a of the adducts. Two peaks were also present at 2.29 and 1.99 ppm (integration 1:0.8, adducts **a** and **b**, respectively in Fig. 6), assignable to the phosphate group of $[\text{Pt}(\text{triphos})(5'\text{-GMP-N7})]$, **6a** and **6b**, as well as a peak due to the free nucleotide. The ^1H NMR spectrum showed two peaks at 8.96 and 8.72 ppm which are shifted to low field compared to the H8 proton resonance of the free nucleotide. Two resonances at 6.15 and 5.82 ppm are assignable to H1' of the sugar moiety of the adducts. The final pH of the solution was *ca.* 4.

The ^{31}P and ^1H NMR spectra of the final solution thus confirm the formation of two different $[\text{Pt}(\text{triphos})(5'\text{-GMP})]$ adducts, in both cases with 5'-GMP bound through the N7 of the guanine base. After the initial formation of the $[\text{Pt}(\text{triphos})(\text{GS})]^+$, **5**, the addition of 5'-GMP in the presence of $\text{Au}(\text{i})$ resulted in the cleavage of the Pt–S bond, and the formation of new Pt–N bonds. Even though the Pt–S bond is generally considered to be inert and difficult to break, recently Cheng and Pai⁵⁸ have described the cleavage of a Pt–S bond from $\text{Pt}(\text{II})\text{-GS}$ adducts in the presence of $\text{Cu}(\text{II})$. In the present case, where all the chloride present in the solution is removed by the AgNO_3 , $\text{Au}(\text{i})$ appears to trigger the displacement of GS by the N atom of the nucleotide.

Reaction of $[\text{Pt}(\text{triphos})\text{Cl}]\text{Cl}$, **2, with *N*-acetyl-L-cysteine.** In the ^{31}P NMR spectrum of the reaction of complex **2** with *N*-acetyl-L-cysteine [1 : 1 molar ratio at *ca.* pH 7.3, $\text{CD}_3\text{OD}\text{-D}_2\text{O}$ (4 : 1), in the presence of AgNO_3], there were two resonances at 46.83 and 92.05 ppm (Table 4), with corresponding coupling constants of 2518 and 2407 Hz. These coupling constants can be assigned to P *trans* to S and P *trans* to $P^{41,42}$ respectively. The resonance at the higher field is assigned to P_a and that at the lower field to P_b . Both signals are shifted to low field, compared to unreacted complex **2**. In the ^1H NMR spectrum peaks due to the $\beta\text{-CH}_2$ of the amino acid were broadened and shifted to low field (by *ca.* 0.6 ppm), indicative of coordination to platinum through the S atom.^{59,60} Thus the ^1H NMR spectrum confirms the formation of $[\text{Pt}(\text{triphos})(\text{AcCys})]^+$, **7**. This adduct has improved water solubility compared to complex **2**, which can be useful for biological purposes.

Reaction of $[\text{Pt}(\text{triphos})\text{Cl}]\text{Cl}$, **2, with *N*-acetyl-L-methionine.** The ^{31}P NMR spectrum of the reaction of complex **2** with *N*-acetyl-L-methionine [1 : 1 molar ratio at *ca.* pH 7.64, $\text{CD}_3\text{OD}\text{-D}_2\text{O}$ (4 : 1), in the presence of AgNO_3] showed the most intense peaks at 77.25, $J(\text{P-Pt}) = 3157$ Hz, and 47.13 ppm, $J(\text{P-Pt}) = 2568$ Hz (Table 4), assignable to P_b and P_a , respectively of the nitrate adduct $[\text{Pt}(\text{triphos})(\text{ONO}_2)]\text{NO}_3$. Two other signals at 95.57 ppm and 94.83 ppm with coupling constants $J(\text{P-Pt}) = 2739$, 2732 Hz, respectively, were also present. These resonances were assigned to P_b , being shifted to low field compared to unreacted complex **2**. The coupling constants are

within the range assigned as P *trans* to S. The spectrum also showed another resonance at 48.36 ppm, which is assigned to P_a. The ¹H NMR spectrum showed peaks at 2.44 and 2.22 ppm assignable to the S-methyl and acetyl protons of the bound amino acid shifted to low field upon coordination through sulfur.⁶¹ This indicates the formation of the monofunctional adduct [Pt(triphos)(AcMet-S)]⁺, **8**.

Reaction of [PtAu(triphos)Cl₃], **4, with thiols.** The reaction of [PtAu(triphos)Cl₃] and GSH in 1:1 molar ratio in DMF–D₂O (4:1) at *ca.* pH 3 (uncorrected meter reading) gave rise to a white precipitate that was filtered off. The ³¹P NMR spectrum of the clear solution showed two peaks at 88.05 ppm, *J*(P–Pt) = 3099 Hz, and 42.99 ppm, *J*(P–Pt) = 2442 Hz, for which reasonable assignments are to P_b and P_a, respectively, of complex **2**, [Pt(triphos)Cl]⁺. After the addition of 2 molar equivalents of GSH in the same solvent system at pH 7.53, the ³¹P NMR spectrum of the reaction mixture showed peaks at 90.60 ppm, *J*(P–Pt) = 2319 Hz, and 45.45 ppm, *J*(P–Pt) = 2559 Hz, these peaks are assigned to P_b and P_a, respectively, of [Pt(triphos)(GS)]⁺ adduct, **5**, which arises from the further reaction of **2** with GSH.

The reaction of [PtAu(triphos)Cl₃], **4** with *N*-acetyl-L-cysteine in 1:1 molar ratio at *ca.* pH 3 in DMF–D₂O (4:1) led to the formation of a white precipitate. After the filtration of the solid, ³¹P NMR spectrum of the solution was recorded (Table 4). It showed two peaks at 88.06 ppm, *J*(P–Pt) = 3095 Hz, and 42.93 ppm, *J*(P–Pt) = 2444 Hz, assignable to P_b and P_a of complex **2**, [Pt(triphos)Cl]Cl, respectively. After the addition of the 2 molar equivalents of amino acid (*ca.* pH 7.21), the ³¹P NMR spectra of the reaction mixture showed two peaks at 90.96 ppm, *J*(P–Pt) = 2292 Hz, and 45.12 ppm *J*(P–Pt) = 2569 Hz. These peaks were assigned to P_b and P_a of [Pt(triphos)(AcCys)]⁺, **7**, respectively. Thus the high affinity of Au(I) for thiolates⁶² dominates reactions of complex **4** with thiols and Au(I) is readily extracted from the bimetallic complexes allowing chelate ring closure.

Conclusion

We have shown that Au(I) can induce chelate ring-opening in Pd(II) and Pt(II) triphos complexes to give novel bimetallic complexes which were shown by X-ray crystallography to contain square-planar Pd(II) and Pt(II) and linear Au(I) centres. It was possible to reverse chelate ring-opening *via* Au(I) abstraction from the bimetallic complex **4**, [PtAu(triphos)Cl₃] using thiols such as the tripeptide glutathione. We also have shown that thiolate adducts of [Pt(triphos)]²⁺ have good aqueous solubility. Substitution of the thiol by the nucleotide 5'-GMP in [Pt(triphos)(GS)]⁺ was observed in the presence of Au(I). These studies provide the basis for further investigation of the biological activity of this class of complexes.

Acknowledgements

We thank Xunta de Galicia (projects XUGA 20903A93 and XUGA 20906A98), Predoctoral Grant for P. S., BBSRC and EPSRC for their support for this work. We also acknowledge assistance of Dr Lesley Yellowlees (The University of Edinburgh) with the use of the electrochemical equipment.

References

- 1 F. A. Cotton and B. Hong, *Prog. Inorg. Chem.*, 1992, **40**, 179.
- 2 S. J. Berners-Price and P. J. Sadler, *Struct. Bonding*, 1988, **70**, 27.
- 3 C. Bolm, D. Kaufmann, S. Gesslers and K. Harms, *J. Organomet. Chem.*, 1995, **502**, 47.
- 4 D. L. DuBois, A. Miedaner and R. C. Haltiwanger, *J. Am. Chem. Soc.*, 1991, **113**, 8753.
- 5 R. E. Rülke, J. G. P. Delis, A. M. Groot, C. J. Elsevier, P. W. N. M. van Leeuwen, K. Vrieze, K. Groubitz and H. Schenk, *J. Organomet. Chem.*, 1996, **508**, 109.

- 6 Y. Yamamoto, T. Tanase, H. Ukaji, M. Hasegawa, T. Igoshi and K. Yoshimura, *J. Organomet. Chem.*, 1995, **498**, C23.
- 7 T. Tanase, H. Toda and Y. Yamamoto, *Inorg. Chem.*, 1997, **36**, 1571.
- 8 K. D. Tan, R. Uriarte, T. J. Mazanec and D. W. Meek, *J. Am. Chem. Soc.*, 1979, **101**, 6614.
- 9 J. Chatt, R. Mason and D. W. Meek, *J. Am. Chem. Soc.*, 1975, **97**, 3826.
- 10 B. Longato, G. Pilloni, G. Valle and B. Corain, *Inorg. Chem.*, 1988, **27**, 956.
- 11 (a) B. Longato, G. Pilloni, G. M. Bonera and B. Corain, *J. Chem. Soc., Chem. Commun.*, 1986, 1478; (b) B. Longato, B. Corain, G. M. Bonera and G. Pilloni, *Inorg. Chim. Acta*, 1987, **137**, 75.
- 12 (a) B. Lippert, *Prog. Inorg. Chem.*, 1989, **37**, 1; (b) B. Lippert, *Gazz. Chim. Ital.*, 1989, **118**, 153 and references therein.
- 13 G. Bandoli, G. Trovo, A. Dolmela and B. Longato, *Inorg. Chem.*, 1992, **31**, 45.
- 14 A. Habtemariam and P. J. Sadler, *Chem. Commun.*, 1996, 1785.
- 15 N. Margiotta, A. Habtemariam and P. J. Sadler, *Angew. Chem., Int. Ed. Engl.*, 1997, **36**, 1185.
- 16 P. Sevillano, A. Habtemariam, A. Castiñeiras, M. E. Garcia and P. J. Sadler, *Polyhedron*, 1998, **18**, 383.
- 17 C. E. Housecroft, B. A. M. Shaykh and A. C. Rheingold, *Acta Crystallogr., Sect. C*, 1990, **46**, 1549.
- 18 E. G. Hope, W. Levason and N. A. Powell, *Inorg. Chim. Acta*, 1986, **115**, 187.
- 19 R. Colton and V. Tedesco, *Inorg. Chim. Acta*, 1992, **202**, 95.
- 20 R. Colton and T. Whyte, *Aust. J. Chem.*, 1991, **44**, 525.
- 21 W. H. Baddley, F. Basolo, H. B. Gray, C. Nölting and A. J. Poë, *Inorg. Chem.*, 1963, **2**, 921.
- 22 S. J. Berners-Price and P. J. Sadler, *Inorg. Chem.*, 1986, **25**, 3822.
- 23 E. F. de Assis and C. A. L. Filgueiras, *Transition Met. Chem.*, 1994, **19**, 484.
- 24 Enraf-Nonius. CAD4-Express Software, Version 5.1, Enraf-Nonius, Delft, The Netherlands, 1995.
- 25 A. L. Spek, HELENA, A Program for Data Reduction of CAD4 Data, University of Utrecht, The Netherlands, 1997.
- 26 A. L. Spek, PLATON, A Multipurpose Crystallographic Tool, University of Utrecht, The Netherlands, 1997.
- 27 G. M. Sheldrick, *Acta Crystallogr., Sect. A*, 1983, **39**, 158.
- 28 G. M. Sheldrick, SHELXL97, Program for the Refinement of Crystal Structures, University of Göttingen, Germany, 1997.
- 29 International Tables for X-ray Crystallography, Kluwer Academic Publishers, Dordrecht, The Netherlands, 1995, vol. C.
- 30 E. Keller, SCHAKAL 92, A Computer Program for the Graphic Representation of Molecular and Crystallographic Models, University of Freiburg, Germany, 1992.
- 31 L. Zsolnai, ZORTEP, A Program for the Presentation of Thermal Ellipsoids, University of Heidelberg, Germany, 1997.
- 32 J. Casier and A. M. Glaze, *J. Appl. Crystallogr.*, 1986, **19**, 205.
- 33 W. Clegg, *Acta Crystallogr., Sect. A*, 1981, **37**, 22.
- 34 G. M. Sheldrick, SHELXTL V. S., Siemens Analytical X-ray instruments, Madison, Wisconsin, 1995.
- 35 D. J. Watkin, C. K. Prout, P. W. Betteridge and J. R. Curruthers, CRYSTALS, Issue 10, Chemical Crystallography Laboratory, University of Oxford, 1996.
- 36 N. Walken and D. Stuart, *Acta Crystallogr., Sect. A*, 1983, **39**, 158.
- 37 R. B. King, P. N. Kapoor and R. N. Kapoor, *Inorg. Chem.*, 1971, **10**, 1841.
- 38 A. K. Al-Sa'ady, C. A. McAullife, R. V. Parish and J. A. Sandbank, *Inorg. Synth.*, 1985, **23**, 191.
- 39 A. Albinati, F. Lianza, H. Berger, P. J. Pregosin, H. Rügger and R. W. Kunz, *Inorg. Chem.*, 1993, **32**, 478.
- 40 W. J. Geary, *Coord. Chem. Rev.*, 1971, **7**, 81.
- 41 A. Handler and P. Peringer, *J. Chem. Soc., Dalton Trans.*, 1990, 3725.
- 42 G. K. Anderson, H. C. Clark and J. A. Davies, *Inorg. Chem.*, 1983, **22**, 434.
- 43 P. E. Garrou, *Chem. Rev.*, 1981, **81**, 229.
- 44 K. D. Tau, R. Uriarte, T. J. Mazanec and D. W. Meek, *J. Am. Chem. Soc.*, 1979, **101**, 6614.
- 45 R. G. Pearson, *Inorg. Chem.*, 1973, **12**, 713.
- 46 W. McFarlane and J. Cass, *J. Chem. Soc., Dalton Trans.*, 1974, 324.
- 47 C. J. Smith, V. S. Reddy and V. Katti, *Chem. Commun.*, 1996, 2557.
- 48 G. I. Bertinsson, *Acta Crystallogr., Sect. C*, 1983, **39**, 563.
- 49 F. H. Allen, O. Kennard and R. Taylor, *Acc. Chem. Res.*, 1983, **16**, 143.
- 50 W. C. Hamilton, *Structural Chemistry and Molecular Biology*, ed. A. Rich and N. Davison, Freeman, San Francisco, 1968, p. 466.
- 51 C. Navarro-Ranninger, F. Zamora, I. Lopez-Solera, A. Mengl and J. R. Masaguer, *J. Organomet. Chem.*, 1996, **506**, 149.
- 52 A. Habtemariam, P. J. Sadler, S. Parsons, A. Castiñeiras, *J. Chem. Soc., Dalton Trans.*, 1999, 2861–2870

- P. Sevallano and M. E. García, 6th International Conference on the Chemistry of the Platinum Group Metals, York, UK, 1996, abstract p. 145.
- 53 A. G. Orpen, L. Brammer, F. H. Allen, O. Kennard, D. G. Watson and R. Taylor, *J. Chem. Soc., Dalton Trans.*, 1989, S69.
- 54 G. K. Anderson and R. Kumar, *Inorg. Chem.*, 1984, **23**, 4064.
- 55 A. Corazza, I. Harvey and P. J. Sadler, *Eur. J. Biochem.*, 1996, **236**, 697.
- 56 O. M. Ni Dhubhghaill, P. J. Sadler and E. García Fernandez, *Metal-Based Drugs*, 1995, **2**, 19.
- 57 L. D. Pettit, K. F. Siddiqui, H. Kozłowski and T. Kowalik, *Inorg. Chim. Acta*, 1981, **55**, 87.
- 58 C.-C. Cheng and C.-H. Pai, *J. Inorg. Biochem.*, 1998, **71**, 109.
- 59 K. J. Barnham, M. I. Djuran, P. S. Murdoch, J. D. Ranford and P. J. Sadler, *Inorg. Chem.*, 1996, **35**, 1065.
- 60 K. J. Barnham, M. I. Djuran, P. S. Murdoch, J. D. Ranford and P. J. Sadler, *J. Chem. Soc., Dalton Trans.*, 1995, 3721.
- 61 K. J. Barnham, Z. Guo and P. J. Sadler, *J. Chem. Soc., Dalton Trans.*, 1996, 2867.
- 62 D. H. Brown and W. E. Smith, *Chem. Soc. Rev.*, 1980, **9**, 217.
- 63 C. K. Johnson, ORTEP, Report ORNL-5138, Oak Ridge National Laboratory, Oak Ridge, TN, 1976.

Paper 9/03775F